IOSR Journal of Applied Physics (IOSR-JAP)
e-ISSN: 2278-4861.Volume 18, Issue 5 Ser. III (Sep. – Oct. 2026), PP 37-49
www.iosrjournals.org

Tuning Structural and Electrochemical properties of Green HPMC-Pectin Solid Polymer Blend Electrolyte through $NaNO_3$ salt suitable for Energy Storage Applications

Nisha K H[1], J. Sannappaa,[1]* Neha K H[2], Rajashekhar F. Bhajatri[2]*, Suhas M Malenahalli[2], Namrata N Mundargi[3]

[1]*Department of PG Studies and Research in Physics, Kuvempu University, Shankaraghatta, Jnanasahyadri, 577451, Karnataka, India*
[2]*Department of Physics, Karnatak University, Dharwad, 580003, Karnataka, India*
[3]*Department of Chemistry, Karnatak University, Dharwad, 580003, Karnataka, India*

Abstract
Green polymer electrolytes have gained considerable attention owing to their potential to improve ionic conductivity and electrochemical stability for sustainable energy-storage applications. In the present study, a solid polymer electrolyte comprising 90 wt.% hydroxypropyl methylcellulose (HPMC), 10 wt.% pectin and 10 wt.%, 20 wt.%, 30 wt.% $NaNO_3$ was successfully fabricated using the solution-casting technique. X-ray diffraction (XRD) analysis revealed the predominantly amorphous nature of the polymer electrolyte even after the incorporation of 10 wt.% $NaNO_3$. Fourier transform infrared (FTIR) spectroscopy confirmed the presence of characteristic functional groups and their interactions within the polymer matrix. Differential scanning calorimetry (DSC) analysis provided insights into the thermal behaviour and glass transition characteristics of the prepared electrolyte. Surface morphological analysis revealed an increase in surface roughness accompanied by randomly distributed nanopores upon salt incorporation. Furthermore, the optimized electrolyte 10 wt.% $NaNO_3$ exhibited a maximum ionic conductivity of 4.70×10^{-5} S cm^{-1}, an electrochemical stability window of 3.1 V, and a maximum cation transference number of 0.765. Dielectric spectroscopic investigations further demonstrated the influence of salt incorporation on the dielectric response and segmental dynamics of the polymer matrix. These results highlight the potential of the developed HPMC/pectin/$NaNO_3$ polymer electrolyte for sustainable electrochemical energy-storage applications.

Keywords: *Biodegradable polymer, Amorphous and flexible, Ionic conductivity, Electrochemical stability window, Transference number*

Date of Submission: 27-10-2026 Date of Acceptance: 18-11-2026

I. Introduction

The increasing demand for efficient, safe, flexible, and environmentally sustainable energy-storage devices has stimulated considerable research interest in the development of solid polymer electrolytes (SPEs) [1][2]. Conventional liquid electrolytes are widely employed in electrochemical energy-storage systems because of their high ionic conductivity. However, their practical applications are often limited by issues such as electrolyte leakage, flammability, chemical instability, and difficulties associated with packaging and long-term operation [3]. Solid polymer electrolytes have emerged as promising alternatives because of their flexibility, lightweight nature, ease of fabrication, improved dimensional stability, and potential for reducing electrolyte leakage. In particular, polymer electrolytes developed from biodegradable and biocompatible materials are gaining attention as environmentally responsible materials for next-generation electrochemical energy-storage applications [4][5].

Polymer electrolytes generally consist of a polymer host and an appropriate ionic salt. The polymer matrix provides mechanical support and contains suitable functional groups that facilitate salt dissolution and ion transport. The ionic salt acts as the source of mobile charge carriers, while interactions between the polymer chains and salt determine the structural, dielectric, and electrical properties of the resulting electrolyte. The ionic conductivity of polymer electrolytes is strongly influenced by salt concentration, polymer–salt interactions, degree of crystallinity, segmental mobility, and the availability of free charge carriers. Therefore, selecting compatible polymer hosts and optimizing salt concentration are essential for obtaining improved electrochemical performance [6][7][8].

Among various biodegradable polymeric materials, hydroxypropyl methylcellulose (HPMC) has attracted considerable interest because of its excellent film-forming ability, water solubility, flexibility, chemical stability, and biocompatibility. HPMC is a cellulose-derived, non-ionic polymer containing hydroxyl and ether functional

groups along its molecular backbone. These functional groups can interact with suitable ionic salts through electrostatic interactions and hydrogen bonding. Its ability to form uniform, transparent, and mechanically stable films makes it a suitable candidate for developing solid polymer electrolytes. Furthermore, the structural characteristics of HPMC provide opportunities for incorporating different ionic salts to modify its electrical and dielectric properties [9][10][11].

Pectin is another naturally occurring polysaccharide that has gained attention as a potential polymer electrolyte host. It is primarily composed of galacturonic acid units containing hydroxyl and carboxyl functional groups. These polar functional groups can participate in interactions with metal ions and influence the dissociation of incorporated salts. Pectin also possesses attractive characteristics, including biodegradability, non-toxicity, renewable availability, and good film-forming properties. However, the electrical and mechanical performance of individual biopolymers may require further improvement for practical electrochemical applications. Combining pectin with another compatible polymer provides an opportunity to modify the structural arrangement, intermolecular interactions, flexibility, and charge-transport characteristics of the resulting polymer matrix [12][13].

Blending HPMC with pectin is therefore an interesting approach to developing environmentally friendly polymer electrolytes. The hydroxyl groups of HPMC and the hydroxyl and carboxyl groups of pectin may establish intermolecular hydrogen-bonding interactions, influencing polymer miscibility and chain organization. Such interactions can modify the degree of crystallinity and segmental mobility of the polymer blend [14][15]. The resulting polymer matrix may provide suitable environments for salt incorporation and ionic transport. Consequently, understanding the structural and electrical interactions between HPMC and pectin is important for optimizing their performance as polymer electrolyte hosts.

The selection of an appropriate ionic salt is another important factor governing the performance of solid polymer electrolytes. Sodium nitrate ($NaNO_3$) is an attractive sodium-ion source because it provides mobile Na^+ ions and nitrate (NO_3^-) counterions. When incorporated into a polymer matrix, the salt can undergo partial or complete dissociation depending on the dielectric environment and interactions between the polymer functional groups and ionic species. The released sodium ions contribute to ionic conduction through the polymer network, while the nitrate ions may interact with the polar groups of the polymer chains [16][17].

The concentration of the incorporated salt plays a significant role in determining the electrical properties of the polymer electrolyte. At relatively low salt concentrations, the number of available mobile charge carriers may be insufficient to produce high ionic conductivity. Increasing the salt concentration can enhance the number of charge carriers and improve conductivity. However, excessive salt incorporation may promote ion association, aggregation, or the formation of ion pairs, thereby reducing the effective number of mobile charge carriers [18][19]. Therefore, an optimum salt concentration is essential for achieving favourable ionic conductivity and dielectric behaviour.

Previous investigations have demonstrated the suitability of $NaNO_3$ for developing sodium-ion-conducting polymer electrolytes. Vahini et al. investigated pectin-based biopolymer electrolytes containing different concentrations of $NaNO_3$ and reported an enhancement in ionic conductivity from (2.7×10^{-9}) to (4.2×10^{-6}) S cm^{-1} upon salt incorporation. Their findings established the potential of pectin as a host polymer for sodium-ion conduction [13]. Similarly, Shetty et al. investigated NaCMC-based solid polymer electrolytes containing $NaNO_3$ and demonstrated the importance of polymer–salt interactions, salt concentration, and ionic mobility in determining the electrical and dielectric response of the electrolyte system [16].

These studies indicate that the incorporation of sodium salts into biodegradable polymer matrices can significantly modify their structural and electrical characteristics. Nevertheless, the performance of an electrolyte depends not only on the salt concentration but also on the chemical nature of the polymer host and the interactions established within the polymer–salt complex.

Although considerable research has been conducted on cellulose derivatives and natural polysaccharides for polymer electrolyte applications, further investigation is required to understand the combined influence of HPMC, pectin and sodium nitrate on the structural, electrical, and dielectric properties of biodegradable polymer blend electrolytes. In particular, the interaction between two chemically different polymer hosts and the concentration-dependent incorporation of $NaNO_3$ may influence salt dissociation, polymer chain organization, ionic mobility, and dielectric relaxation behaviour.

In this context, the present investigation focuses on the development of HPMC/pectin-based sodium-ion-conducting solid polymer electrolyte films containing different concentrations of $NaNO_3$ through the solution-casting technique. The influence of sodium nitrate concentration on the structural characteristics, polymer–salt interactions, ionic conductivity and dielectric properties is systematically investigated. The prepared electrolyte films are expected to provide insights into the relationship between polymer–salt complexation and charge-transport mechanisms.

The principal objective of this investigation is to identify the optimum $NaNO_3$ concentration that produces favourable structural and electrical characteristics in the HPMC/pectin polymer blend. The study also aims to

establish the suitability of these biodegradable polymer-based electrolyte films for potential applications in environmentally sustainable electrochemical energy-storage devices.

Preparation of Solid Polymer Electrolytes

The solid polymer electrolyte (SPE) films were prepared by the solution casting technique. Initially, 90 wt.% of Hydroxypropyl Methylcellulose (HPMC) and 10 wt.% of pectin were accurately weighed and dissolved in distilled water in a 100 mL beaker. For salt-incorporated samples, appropriate amounts of sodium nitrate corresponding to 10 wt.%, 20 wt.%, and 30 wt.% of the total polymer weight were added to the polymer solution to obtain N10, N20 and N30 compositions respectively, while the salt-free film was designated as N0. The resulting mixtures were continuously stirred using a magnetic stirrer at 350 rpm for 12 h to ensure complete dissolution of the polymers and uniform dispersion of the salt throughout the polymer matrix. The beaker was covered with aluminium foil during stirring to prevent contamination and minimize solvent evaporation. After obtaining a clear, homogeneous, and bubble-free solution, the mixture was cast onto a clean, levelled Petri dish and dried in a hot-air oven at 55 °C for 24 h to remove the solvent and facilitate film formation. The dried films were then carefully peeled off from the casting surface and stored in a desiccator to avoid moisture absorption before further characterization.

Characterization techniques

The structural properties of optimized solid polymer electrolytes were investigated by X-Ray Diffractometer (Rigaku SmartLab, Japan) with Cu-K (1.5406 A°) radiation in the 2θ range of 10° to 80° with an step size of 0.01°. The molecular structure and interactions among polymer chains in the polymer blend electrolytes were analyzed using ATR-FTIR data from a Shimadzu FTIR Spectrophotometer (IR Spirit-T) in the wavenumber range of 4000 to 400 cm^{-1}. Additionally, DSC curves from a Hitachi Thermal Analysis System were used to evaluate the glass transition temperature, and phase transitions of the solid polymer electrolyte (SPEs) across a temperature range from ambient to 400°C with a heating rate of 4°C per minute. The image processing technique on a 2D scanning electron microscopy (SEM) picture of the polymer composites shows the distribution of morphological structures and their agglomerates. An SEM (JSM 6360; JEOL) with a 5 kV applied potential and multiple resolutions was used to analyze the surface morphology and elemental composition of the composites. EIS was carried out to understand how dopant concentration affects ionic conductivity. A HIOKI IM3570 Impedance Analyzer was used for the measurements. To prevent ion passage, the specimens were placed between stainless steel electrodes (S.S/SPE/S. S, grade 304). The sample was exposed to an alternating current (AC) voltage of 500 mV with a frequency range of 4Hz to 5MHz. The dielectric and Electric modulus were calculated based on Impedance data. Linear Sweep voltammetry was measured up to 5V with a step size of 2 mV/s and measured the current density by Origalys Electrochemical workstation (OGF+500, France) by sandwiching 14mm circular polymer film in a Swagelok type stainless steel electrodes.

II. Result and discussion

XRD

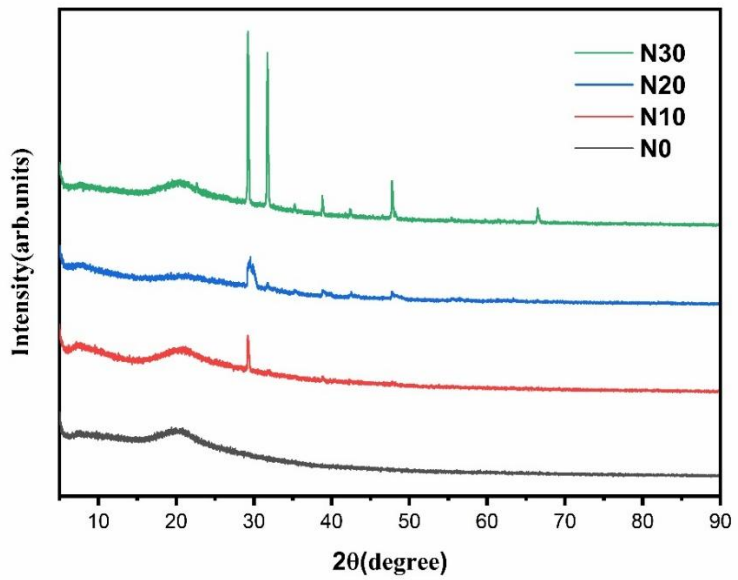

Figure 1. Diffraction pattern of HPMC-pectin based solid polymer electrolytes across different compositions labeled N0, N10, N20 and N30.

The X-ray diffraction patterns of HPMC–pectin-based solid polymer electrolytes (N0, N10, N20 and N30) demonstrate the influence of $NaNO_3$ incorporation on the structural ordering of the polymer matrix. The pristine polymer blend (N0) exhibits a broad diffraction halo centred around 20–22°, indicating its predominantly amorphous nature [20]. Following the incorporation of $NaNO_3$, distinct crystalline reflections emerge, particularly in the N10, N20 and N30 compositions. The observed reflections can be compared with the characteristic diffraction peaks of trigonal $NaNO_3$, corresponding to the (104), (006), (110), (113), (202) and (018) crystallographic planes, occurring approximately at 2θ values of 29.4°, 31.8°, 35.4°, 38.9°, 42.5° and 48.0°, respectively. The increasing prominence of these reflections with salt concentration indicates a greater contribution from crystalline salt-rich domains within the polymer matrix. Meanwhile, the persistence of the broad amorphous halo suggests that the polymer phase retains its disordered structure. This coexistence of amorphous polymer regions and crystalline $NaNO_3$-rich domains demonstrates the structural modifications induced by salt incorporation [21][22]. At higher salt concentrations, the formation of crystalline domains may indicate partial salt aggregation or recrystallization due to limited salt-dissolution capacity of the polymer matrix. These structural changes are expected to influence polymer segmental mobility and ionic transport behaviour [23].

FTIR

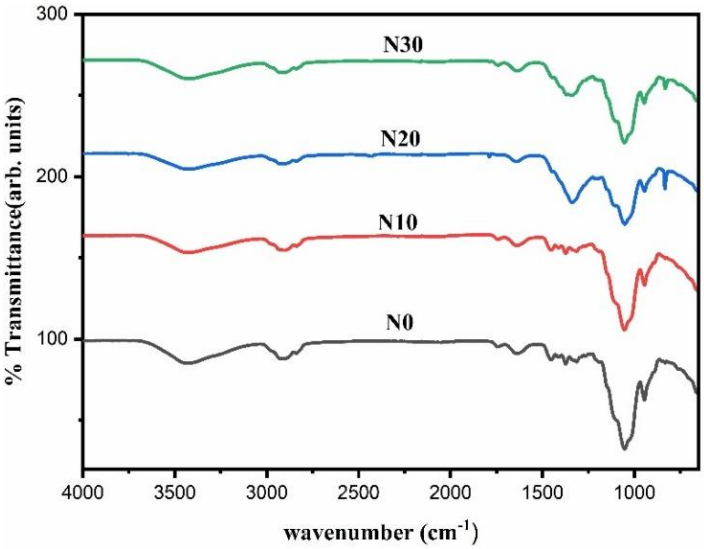

Figure 2. FTIR band assignments of N0, N10, N20, N30 Solid polymer electrolytes

Figure 2 illustrates the FTIR spectra of HPMC–pectin-based solid polymer electrolyte films containing different concentrations of $NaNO_3$ (N0, N10, N20 and N30) and the corresponding functional group assignments is given in Table 1. The spectra provide evidence of the functional groups involved in the polymer matrix and their interactions following salt incorporation. The broad absorption band observed in the 3200–3550 cm^{-1} region is attributed to O–H stretching vibrations of hydroxyl groups present in HPMC and pectin. The broadening of this band is associated with the formation of intermolecular hydrogen bonding within the polymer matrix. The absorption feature around 2980 cm^{-1} corresponds to aliphatic C–H stretching vibrations of the polymer chains. A characteristic band near 1637 cm^{-1} is associated with the bending vibration of absorbed water molecules and may also contain contributions from carboxylate-related vibrations of pectin. The absorption features in the 1400–1450 cm^{-1} region are mainly attributed to symmetric stretching vibrations of carboxylate (COO^-) groups. Furthermore, the bands appearing in the 1000–1350 cm^{-1} region are associated with C–O and C–O–C stretching vibrations of the polysaccharide backbone [24][25][26].

Upon the addition of $NaNO_3$, modifications in the intensity, shape and position of certain absorption bands indicate changes in the molecular environment of the polymer functional groups. In particular, the oxygen-containing groups, such as hydroxyl, carboxylate and ether functionalities, can interact with Na^+ ions through ion–dipole interactions and coordination. These interactions modify the existing hydrogen-bonding network and influence the local chemical environment of the polymer chains. Additionally, characteristic nitrate-ion vibrations may contribute to the absorption features around 1380–1400 cm^{-1} and approximately 830 cm^{-1}. The observed spectral changes collectively support the incorporation of $NaNO_3$ into the HPMC–pectin polymer matrix and the establishment of polymer–salt interactions. Such interactions are important because they influence the structural organization and segmental dynamics of the polymer chains, which are closely related to ionic transport in solid polymer electrolytes [16][27].

Table 1. ATR FTIR bands and assignment of functional groups.

Observed FTIR bands (cm^{-1}) for optimized electrolytes				Band Assignments
N0	N10	N20	N30	
3200-3550	3200-3550	3200-3550	3200-3550	O-H stretching
2932	2932	2924	2917	C-H stretching
1637	1628	1637	1644	C=O stretching
1450	1443	1450	1443	COO^- stretching
1227	1227	1242	1219	C-O stretching
1055	1041	1048	1048	C-O stretching
830	839	846	850	NO_3^-

DSC

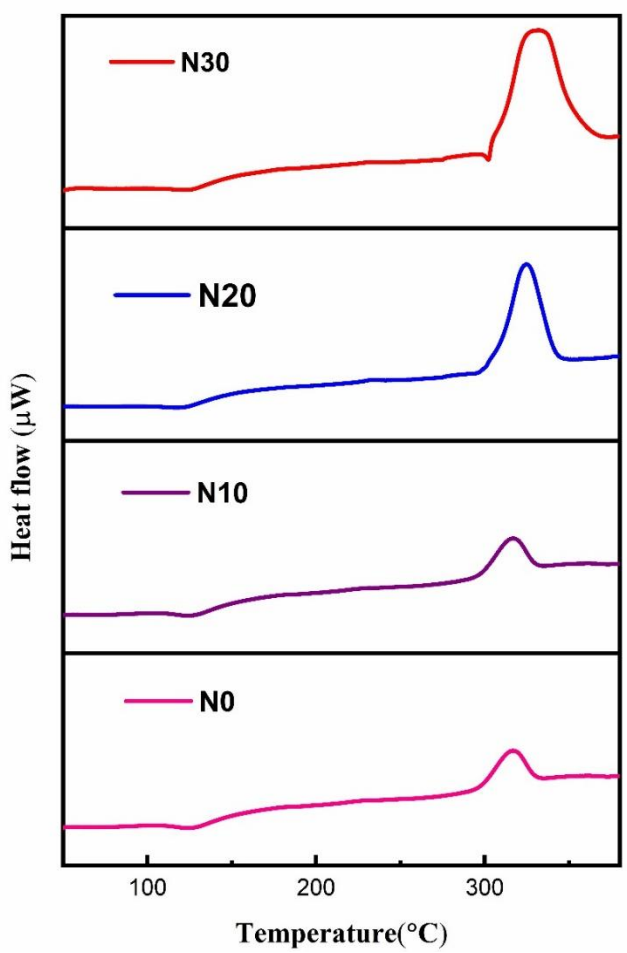

Figure 3. DSC thermograms of N0, N10, N20, N30 Solid polymer electrolytes

Figure 3 illustrates the DSC thermograms of HPMC–pectin-based solid polymer electrolyte films containing different concentrations of $NaNO_3$ (N0, N10, N20 and N30) recorded over a temperature range of approximately 0–380°C. The thermograms exhibit distinct thermal features associated with the thermal transitions and degradation behaviour of the polymer electrolyte system. In general, the glass transition temperature (T_g) of hydrophilic polymer-based electrolyte systems may occur over a broad temperature range of approximately 50–150°C depending on polymer composition, molecular interactions and moisture content. In the present thermograms, a minor baseline variation is observed approximately in the 120–150°C region, which may be associated with moisture-related thermal changes and possible glass-transition behaviour [28][29]. However, a distinct glass transition step is not clearly resolved. A broad thermal event in this region may also be attributed to the removal of absorbed moisture and residual water molecules due to the hydrophilic nature of HPMC and pectin. Furthermore, a prominent thermal peak is observed in the higher-temperature region of approximately 315–340°C for all compositions, which may be associated with the major thermal degradation process of the polymer matrix, involving the breakdown of glycosidic linkages and other thermally sensitive functional groups. The apparent shift of this high-temperature peak towards higher temperatures with increasing $NaNO_3$ concentration suggests modifications in the thermal response of the polymer electrolyte films. This behaviour may be related to

interactions between Na^+ ions and oxygen-containing functional groups, such as hydroxyl, ether and carboxylate groups, which influence the molecular environment of the polymer chains. Overall, the DSC results indicate that $NaNO_3$ incorporation modifies the thermal behaviour of the HPMC–pectin polymer matrix and influences its thermal transitions and high-temperature degradation characteristics [30][31].

Electrochemical impedance spectroscopy (EIS)

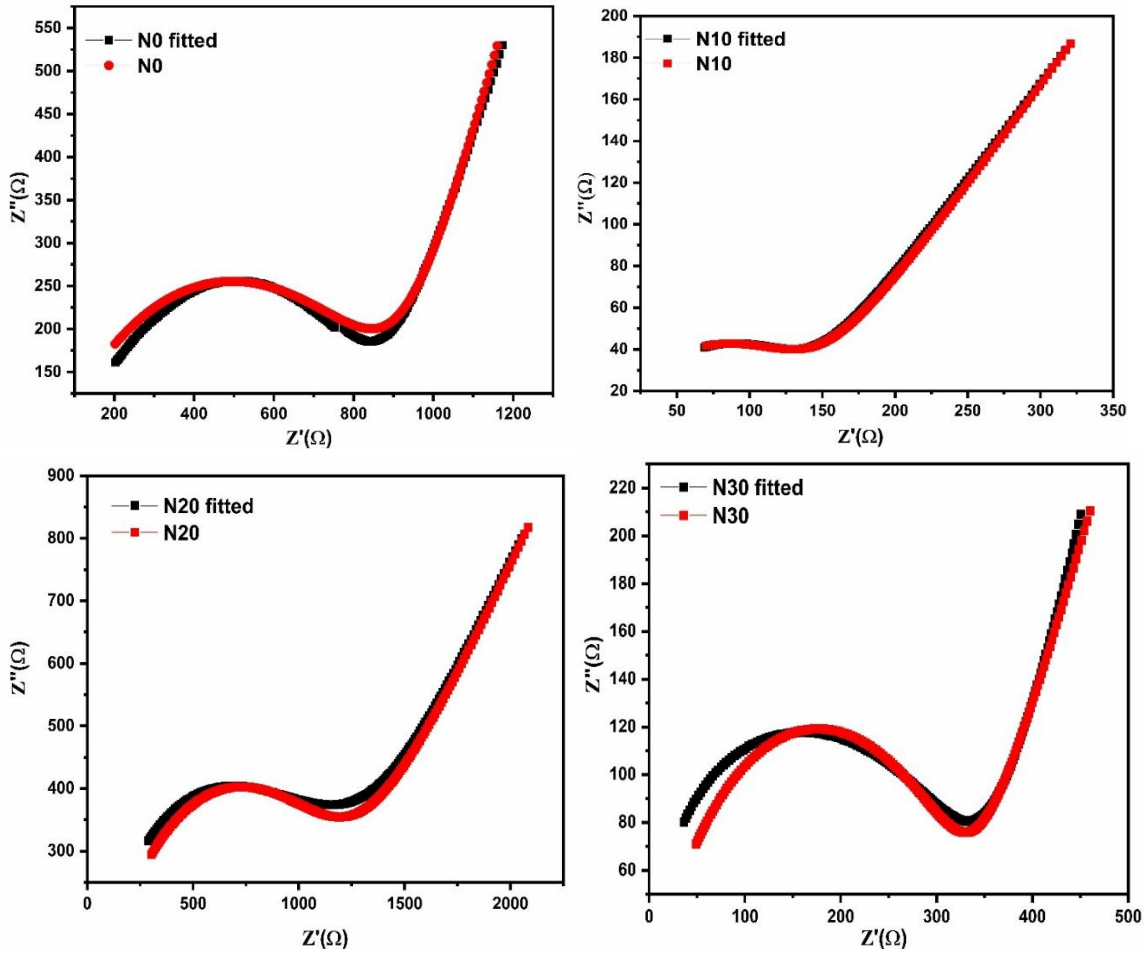

Figure 4. Nyquist plots of N0, N10, N20, and N30 solid polymer electrolyte films showing the experimental impedance data and corresponding fitted curves.

Figure 4 shows the Nyquist plots (Z″ versus Z′) of HPMC–pectin polymer electrolyte films containing different concentrations of $NaNO_3$, together with their fitted curves. The close overlap between the experimental and fitted data confirms the suitability of the equivalent circuit model used for analyzing the electrical behaviour of the polymer electrolytes.

The bulk conductivity (in S cm^{-1}) is evaluated by the following equation (1)

$$\sigma_{dc} = \frac{d}{R_b A} \quad (1)$$

Where d is the polymer film thickness and A is the contact area. The bulk resistance, thickness and ionic conductivity are tabulated in Table 2.

The impedance spectra of all samples consist of a depressed semicircle in the high-frequency region followed by an inclined spike at lower frequencies. The depressed semicircle is associated with the bulk response of the polymer electrolyte and originates from the combined effect of ionic conduction and dielectric relaxation within the material. The low-frequency spike is attributed to electrode polarization caused by the accumulation of charge carriers at the electrode–electrolyte interface, indicating the predominantly ionic nature of conductivity[32].

For the pristine HPMC–pectin film (N0), a comparatively large semicircle is observed, indicating higher bulk resistance and lower ionic conductivity. The larger diameter of the semicircle suggests limited mobility of charge carriers within the polymer matrix due to the absence of additional salt ions. Upon the incorporation of 10 wt.% $NaNO_3$ (N10), the diameter of the semicircle decreases significantly, indicating a substantial reduction in bulk resistance. This behaviour can be attributed to the dissociation of $NaNO_3$ within the polymer host, which increases the concentration of mobile Na^+ ions and facilitates ion transport through the polymer network. The reduced

resistance demonstrates improved ionic conductivity compared with the undoped sample. For the N20 sample, the semicircle diameter increases relative to N10, suggesting an increase in bulk resistance. This behaviour may arise from ion association or partial ion aggregation at higher salt concentrations, which reduces the number of free charge carriers available for conduction and restricts polymer chain mobility. The N30 sample exhibits a semicircle diameter smaller than that of N20 but larger than that of N10, indicating moderate bulk resistance. The presence of the inclined spike at low frequencies confirms the continued dominance of ionic conduction and electrode polarization effects. The slight improvement in conductivity compared with N20 may result from enhanced salt dissociation and increased amorphous regions within the polymer matrix. The bulk resistance (R_b) of the polymer electrolyte can be estimated from the intercept of the semicircle on the real impedance axis (Z′) [33–35].

The reduction in resistance observed for N10 indicates that 10 wt.% $NaNO_3$ provides an optimum balance between ion concentration and polymer chain flexibility, resulting in enhanced ion transport. Therefore, N10 can be considered the most electrically conductive composition among the investigated samples.

Table 2. Values of bulk resistance obtained by EEC modelling (R_b), Bulk conductivity of N0, N10, N20, and N30 solid polymer electrolytes

Sample	Thickness (μm)	$R_b(\Omega)$	σ_{dc}(S cm^{-1})
N0	55.5	909.99	4.60×10^{-6}
N10	82	131.54	4.70×10^{-5}
N20	84.2	1038.00	6.11×10^{-6}
N30	101	321.67	2.37×10^{-5}

Dielectric properties

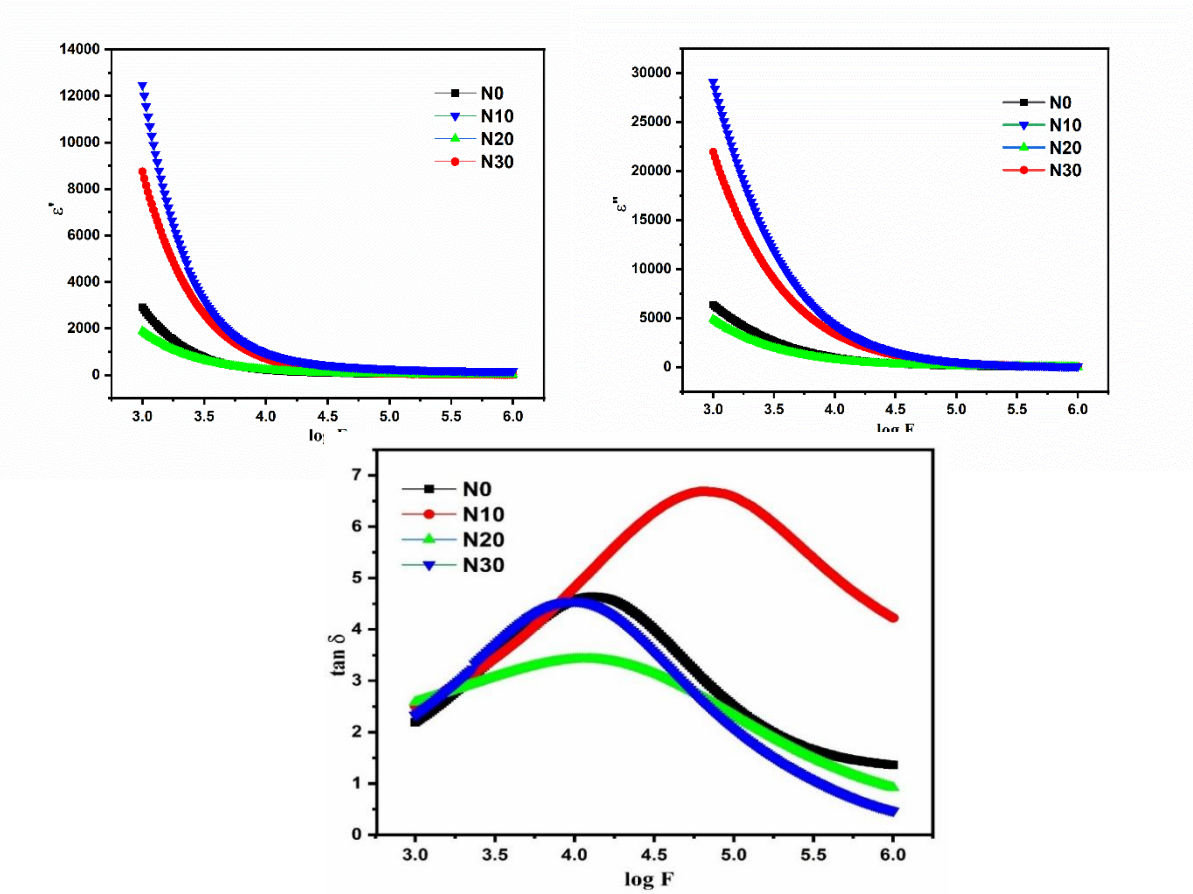

Figure 5. (a)ε' vs. log F (b) ε'' vs. log F and (c) tan δ vs. log F of N0, N10, N20, and N30 solid polymer electrolyte

The dielectric characteristics of an electrolyte are vital for enhancing the performance of energy storage devices. Key parameters such as the dielectric constant (ε'), dielectric loss (ε"), tan loss (tan δ) electrolyte are determined using equations

$$\varepsilon' = \frac{-Z''}{\omega C_0 (Z'+Z'')^2} \quad (2)$$

$$\varepsilon'' = \frac{Z'}{\omega C_0 (Z'+Z'')^2} \quad (3)$$

$$\tan\delta = \frac{\varepsilon''}{\varepsilon'} \quad (4)$$

where Z' and –Z" represent the impedance values derived from Nyquist plots, and ω_{peak} is the angular frequency identified as the point of maximum loss on the tan δ curve and the dielectric plots were illustrated in Figure 5a-5c.

The variation of the dielectric constant (ε') with frequency for HPMC-pectin-based polymer electrolytes containing different concentrations of $NaNO_3$ is shown in figure 5(a). For all samples, ε' decreases sharply with increasing frequency and gradually reaches a nearly constant value at higher frequencies. This behaviour is characteristics of polymer electrolytes and can be attributed to the inability of dipoles and mobile ions to follow the rapidly alternating electric field at high frequencies. At lower frequencies, a large dielectric constant is observed due to the accumulation of charge carriers at the electrode-electrolyte interface, resulting in strong electrode polarization and space-charge effects. The addition of $NaNO_3$ significantly influences the dielectric response of the polymer matrix. Among all compositions, the N30 sample exhibits the highest dielectric constant, followed by N10, N0 and N20. The enhanced ε' valve for N30 suggests increased ion dissociation and a larger concentration of mobile charge carriers with in the polymer host. The higher dielectric constant indicates improved polarization capability and stronger ion-polymer interactions. The N20 sample shows comparatively lower ε' values, suggesting a reduction in affective polarization, possibly due to ion aggregation or restricted segmental motion of the polymer chains [36–38].

Figure 5(b) illustrates the frequency dependence of the dielectric loss (ε″) for the prepared polymer electrolyte films. Similar to ε′, the dielectric loss decreases continuously with increasing frequency for all samples. The high ε″ values observed in the low-frequency region arise from charge carrier migration and electrode polarization effects, which contribute significantly to energy dissipation. The N30 sample exhibits the highest dielectric loss, followed by N10, N0, and N20. The increase in ε″ with $NaNO_3$ concentration indicates a greater number of free ions participating in the polarization process. At higher frequencies, the dielectric loss decreases substantially because the charge carriers are unable to respond effectively to the rapidly oscillating electric field. The reduction in dielectric loss at high frequencies reflects the suppression of interfacial polarization and confirms the frequency-dependent relaxation behaviour of the polymer electrolyte system[27,39].

The variation of dielectric loss tangent (tan δ) with frequency is presented in Figure 5(c). All samples exhibit broad relaxation peaks indicating non-Debye relaxation behaviour commonly observed in polymer electrolyte systems. The presence of broad peaks suggests a distribution of relaxation times arising from the heterogeneous nature of the polymer matrix and ion–polymer interactions. The N10 sample displays the highest tan δ peak, reaching a maximum value near log F ≈ 4.8, indicating stronger dielectric relaxation and enhanced ionic mobility compared with the other compositions. The N0 and N30 samples show relaxation peaks around log F ≈ 4.0, whereas N20 exhibits a broader and less intense peak. The shift of the relaxation peak toward higher frequencies for N10 suggests a shorter relaxation time and faster polarization response of the charge carriers. Such behaviour indicates improved ion transport within the polymer matrix due to the optimum concentration of $NaNO_3$ [27,40].

Overall, the dielectric studies reveal that the incorporation of $NaNO_3$ modifies the polarization and relaxation characteristics of the HPMC–pectin polymer electrolyte. The N10 composition exhibits the highest dielectric constant and dielectric loss, reflecting increased charge carrier concentration, while the N10 sample demonstrates the most pronounced relaxation behaviour, indicating favourable ion mobility and enhanced dielectric performance.

SEM

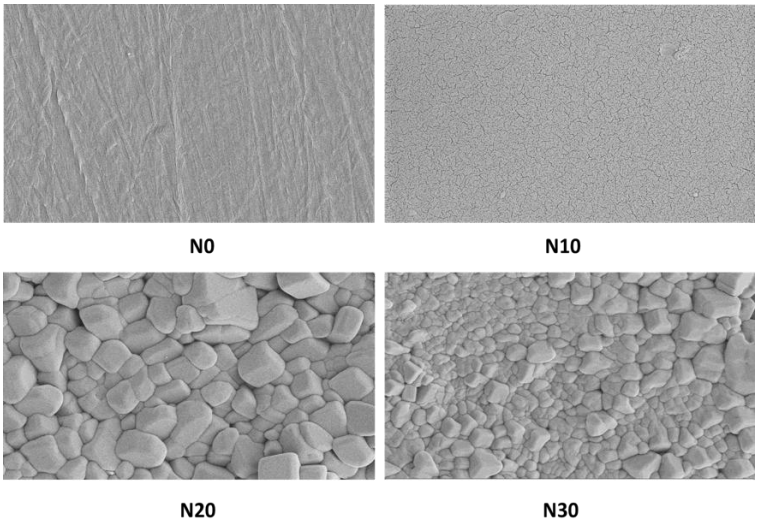

Figure 6. SEM images of N0, N10, N20, and N30 solid polymer electrolyte

The surface morphology of HPMC–pectin films containing different concentrations of $NaNO_3$ (0–30%) was examined using scanning electron microscopy (SEM), and the corresponding micrographs are shown in a Figure 6.

The N0 sample (HPMC + pectin without $NaNO_3$) exhibited a relatively continuous, compact, and homogeneous surface morphology with no obvious particulate structures or phase separation. The smooth appearance suggests good compatibility and intermolecular interaction between HPMC and pectin, resulting in the formation of a uniform polymeric matrix. Upon incorporation of 10 wt.% $NaNO_3$ (N10), noticeable changes in morphology were observed. The SEM image revealed the appearance of discrete crystal-like domains with irregular and elongated particle shapes distributed over the surface. This indicates that the addition of $NaNO_3$ disrupted the initially smooth polymer network and promoted localized salt aggregation or partial crystallization within the HPMC–pectin matrix. The heterogeneous surface suggests incomplete dispersion of salt at this concentration [41].

For the N20 sample, the surface became more densely packed and consisted of larger agglomerated granular structures with improved surface coverage compared with N10. The reduction in empty spaces and the development of interconnected domains imply stronger interactions between the polymer chains and $NaNO_3$ ions. The morphology indicates that salt incorporation enhanced structural rearrangement and produced a more consolidated matrix. At the highest loading, N30 displayed a highly compact and closely packed granular morphology composed of smaller particles with reduced interparticle spacing. The increased particle density and reduced feature size suggest that higher $NaNO_3$ concentration promoted nucleation and more uniform distribution of salt-related domains throughout the polymer matrix. However, the increased roughness and crowded microstructure may also indicate partial saturation of the polymer network and the onset of aggregation due to excessive salt content [42,43].

Overall, the SEM observations demonstrate that increasing $NaNO_3$ concentration significantly altered the morphology of the HPMC–pectin system, transforming the structure from a smooth and homogeneous polymer surface (N0) to a progressively granular and compact morphology (N10–N30). These changes indicate enhanced interaction between $NaNO_3$ and the polymer matrix and may influence properties such as ionic transport, mechanical behaviour, and film stability.

Linear sweep Voltammetry

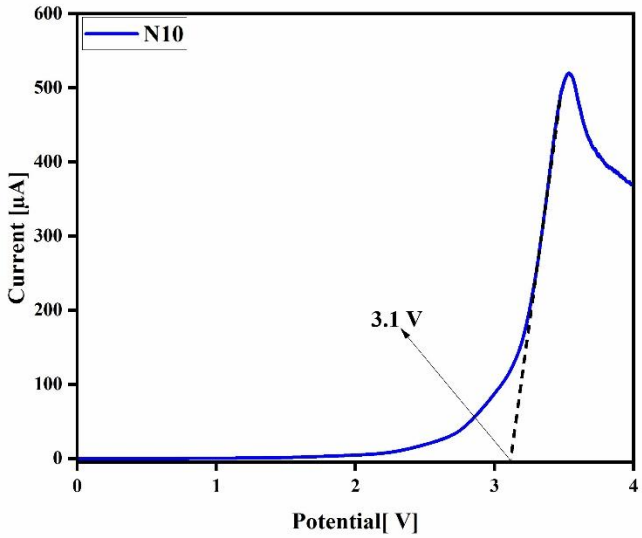

Figure 7. Linear sweep Voltammetry of highest conducting solid polymer electrolyte N10.

The LSV response of the N10 electrolyte exhibits a relatively low and nearly constant current at lower applied potentials, indicating that the electrolyte remains electrochemically stable within this potential region as shown in Figure 7. As the applied potential increases, a gradual rise in current is observed, followed by a pronounced increase at approximately 3.1 V. The potential of 3.1 V, determined by extrapolating the sharply rising current region towards the baseline, represents the approximate onset potential for oxidative decomposition of the electrolyte[44,45]. This indicates that the polymer electrolyte maintains electrochemical stability up to approximately 3.1 V.

Beyond this potential, the current increases rapidly and reaches a maximum value of approximately 530 μA at around 3.6 V. This substantial increase in current is associated with oxidation-related electrochemical reactions and possible decomposition of the electrolyte components. The subsequent decrease in current at higher potentials may be related to changes in the electrode–electrolyte interfacial response or polarization effects[46,47].

Overall, the N10 solid polymer electrolyte exhibits an electrochemical stability window of approximately 3.1 V, suggesting its potential suitability for electrochemical energy-storage applications. The observed stability indicates that the electrolyte can withstand an applied potential up to approximately 3.1 V before significant oxidative reactions begin.

Chronoamperometric studies

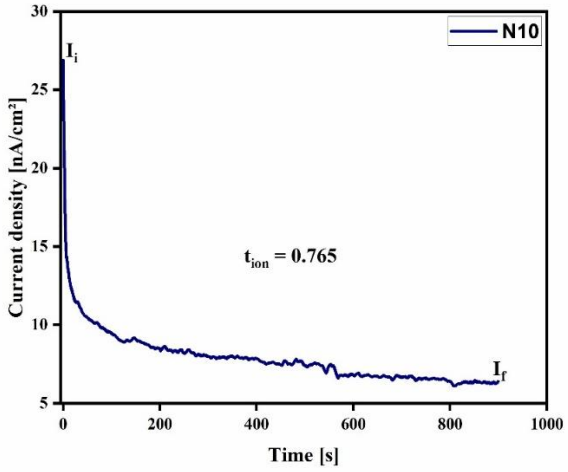

Figure 8. Chronoamperometric plot of the highest conducting solid polymer electrolyte N10.

The graph 8 illustrates the variation of current density with time for the N10 solid polymer electrolyte, obtained through a DC polarization measurement. This analysis provides information about the ionic transport behaviour and the contribution of mobile ions to the total charge transport within the polymer electrolyte. Initially, a relatively high current density is observed (approximately 27 nA cm^{-2}), which is attributed to the movement of mobile ionic species under the applied electric field [48]. As polarization proceeds, the current density decreases rapidly, followed by a gradual reduction towards a nearly stable value. This initial decrease is associated with the redistribution and accumulation of mobile ions near the electrode–electrolyte interfaces, resulting in the development of concentration polarization [49]. Subsequently, the current approaches a steady-state value (approximately 6–7 nA cm^{-2}), indicating the establishment of a relatively stable polarization condition. The residual current at the steady state is generally associated with the contribution of electronic charge transport and any remaining non-ionic current [50].

The ionic transference number (t_{ion}) was determined from the initial (I_i) and steady-state (I_s) currents using the following relationship:

$$t_{ion}=\frac{I_i - I_s}{I_i} \quad (5)$$

Where I_i represents the initial current and I_s represents the steady-state current obtained after polarization. The calculated ionic transference number for the N10 electrolyte was found to be 0.765, indicating that approximately 76.5% of the total current contribution is associated with ionic transport, while the remaining 23.5% represents the estimated electronic contribution under the measurement conditions. The relatively high ionic transference number suggests that the N10 polymer electrolyte exhibits predominantly ionic charge transport, which is desirable for its application in solid-state electrochemical energy-storage devices. This behaviour indicates the effective participation of mobile ionic species in the polymer matrix and supports the potential suitability of the developed electrolyte for electrochemical applications [51].

III. Conclusion

In conclusion, the present investigation demonstrates the successful development of a sustainable HPMC/pectin-based solid polymer electrolyte incorporated with $NaNO_3$, offering a promising approach towards the advancement of biodegradable electrochemical energy-storage materials. The incorporation of $NaNO_3$ effectively modified the structural arrangement and dielectric response of the polymer matrix while retaining its predominantly amorphous character, thereby facilitating favourable conditions for ionic transport. The optimized electrolyte achieved an ionic conductivity of 4.70×10^{-5} S cm^{-1}, a cation transference number of 0.765, and an electrochemical stability window of 3.1 V, demonstrating its promising electrochemical characteristics. The observed dielectric behaviour further highlights the significance of frequency-dependent polarization and molecular relaxation in governing the ionic transport mechanism. More importantly, the combined contribution of HPMC, pectin and $NaNO_3$ establishes a potential pathway for designing environmentally responsible polymer electrolyte systems. This study not only emphasizes the importance of biopolymer–salt interactions in tailoring electrolyte performance but also provides a foundation for developing flexible, sustainable, and potentially biodegradable electrolyte materials for next-generation electrochemical energy-storage devices.

CRediT authorship contribution statement

Nisha K H: Writing – original draft, Software, Methodology, Investigation, Data curation, Conceptualization. J. Sannappa: Writing – review & editing, Visualization, Validation, Supervision, Resources, Investigation, Conceptualization. Neha K H: Writing – original draft, Methodology, Investigation, Conceptualization. Rajashekhar F. Bhajantri: Formal analysis, Validation, Supervision. Suhas M: original draft, Methodology. Namrata N Mundargi: Resources.

Declaration of competing interest

The authors declare that they have no known competing financial interests or personal relationships that could have appeared to influence the work reported in this paper.

Submission Declaration

The authors declare that the manuscript is our original work and all the authors contributed significantly. Further, this work is not been previously published and not under consideration elsewhere.

References

[1] F. Javanbakht, M.R. Saeb, M. Salami-Kalajahi, Renewable Polymer Electrolytes: Toward Sustainable Wearable Energy Devices, Adv. Ind. Eng. Polym. Res. (2026).

[2] X. Fan, C. Zhong, J. Liu, J. Ding, Y. Deng, X. Han, L. Zhang, W. Hu, D.P. Wilkinson, J. Zhang, Opportunities of flexible and portable electrochemical devices for energy storage: expanding the spotlight onto semi-solid/solid electrolytes, Chem. Rev. 122 (2022) 17155–17239.

[3] P.U. Nzereogu, A. Oyesanya, S.N. Ogba, S.O. Ayanwunmi, M.S. Sobajo, V.C. Chimsunum, V.O. Ayanwunmi, M.O. Amoo, O.T.

Adefemi, C.C. Chukwudi, Solid-State lithium-ion battery electrolytes: Revolutionizing energy density and safety, Hybrid Adv. 8 (2025) 100339.
[4] L. Zhu, H. Yang, K. Liu, W. Li, Y. Tang, X. Li, T. Xu, L. Dai, C. Si, Molecularly engineered cellulose: the next-generation sustainable polymer electrolyte material, Energy Environ. Sci. 19 (2026) 1407–1457.
[5] D.R.L.M. REDDY, Development and Characterization of Biodegradable Polymer Electrolytes for High-Performance Solid-State Energy Storage Applications, Int. J. Econ. Soc. Sci. Manag. LAW 6 (2025) 71–85.
[6] V. Prasannavenkadesan, V. Katiyar, A.S. Achalkumar, Polymer electrolytes: evolution, challenges, and future directions for lithium-ion batteries, RSC Appl. Polym. 3 (2025) 499–531.
[7] M. Paillot, G. Foran, A. Prébé, M. Dollé, Mapping Salt Distribution and Ion Mobility in Mixed-Polymer Electrolytes for Solid-State Batteries Using Nuclear Magnetic Resonance Spectroscopy, Chem. Mater. (2026).
[8] L.P. Teo, M.H. Buraidah, A.K. Arof, Development on solid polymer electrolytes for electrochemical devices, Molecules 26 (2021) 6499.
[9] R.-A. Vlad, A. Pintea, C. Pintea, E.-M. Rédai, P. Antonoaea, M. Bîrsan, A. Ciurba, Hydroxypropyl methylcellulose—a key excipient in pharmaceutical drug delivery systems, Pharmaceutics 17 (2025) 784.
[10] E.A. Ozon, A.M. Burloiu, A.M. Musuc, G. Manda, V. Anuta, C.E. Dinu-Pîrvu, D. Lupuliasa, I.V. Neagoe, M. Anastasescu, R.P. Socoteanu, Cellulose-derived gels for topical delivery: HPMC as a functional matrix for porphyrinic photosensitizers, Gels 11 (2025) 824.
[11] N.S. Rani, J. Sannappa, T. Demappa, Mahadevaiah, Structural, thermal, and electrical studies of sodium iodide (NaI)-doped hydroxypropyl methylcellulose (HPMC) polymer electrolyte films, Ionics (Kiel). 20 (2014) 201–207.
[12] M. Muthukrishnan, C. Shanthi, S. Selvasekarapandian, R. Manjuladevi, P. Perumal, P. Chrishtopher Selvin, Synthesis and characterization of pectin-based biopolymer electrolyte for electrochemical applications, Ionics (Kiel). 25 (2019) 203–214.
[13] M. Vahini, M. Muthuvinayagam, M.I.N. Isa, Preparation and characterization of biopolymer electrolytes based on pectin and NaNO3 for battery applications, Polym. Sci. Ser. A 61 (2019) 823–831.
[14] N.A. Ramli, F. Adam, K.N. Mohd Amin, N.F. Abu Bakar, M.E. Ries, Mechanical and thermal evaluation of carrageenan/hydroxypropyl methyl cellulose biocomposite incorporated with modified starch corroborated by molecular interaction recognition, ACS Appl. Polym. Mater. 5 (2023) 182–192.
[15] B. Kocaağa, F.S. Güner, Influence of plasticizer type on the structure and drug release characteristics of LM-pectin hydrogels, Turkish J. Chem. 50 (2026) 1–11.
[16] S.K. Shetty, Ismayil, S. Hegde, V. Ravindrachary, G. Sanjeev, R.F. Bhajantri, S.P. Masti, Dielectric relaxations and ion transport study of NaCMC: NaNO3 solid polymer electrolyte films, Ionics (Kiel). 27 (2021) 2509–2525.
[17] S. Kumar, R. Raghupathy, M. Vittadello, Sodium Polymer Electrolytes: A Review, Batteries 10 (2024) 73. https://doi.org/10.3390/batteries10030073.
[18] R.M. Bueno, L.A. Cordeiro, E.V. Silva, C. das D. do Nascimento, E.G. Souza, J. Marini, N.L.V. Carreno, A.L. Missio, R. de A. Delucis, C.M. Cholant, Enhancing ionic transport in green gel polymer electrolytes based on alginate/lignin/Na2SO4 systems, ACS Omega 11 (2026) 31778–31791.
[19] A. Arya, A.L. Sharma, Effect of salt concentration on dielectric properties of Li-ion conducting blend polymer electrolytes, J. Mater. Sci. Mater. Electron. 29 (2018) 17903–17920.
[20] A.K. Saleh, H. Alenezi, J.S. Albrahim, F.F. Hong, Dual-functional xanthan gum/chitosan nanocomposite doped with copper oxide nanoparticles for high-capacity adsorption of methylene blue and methyl orange dyes and antimicrobial applications, RSC Adv. 16 (2026) 47028–47044.
[21] V. Cyriac, Ismayil, I.S.B.M. Noor, Z.E. Rojudi, Y.N. Sudhakar, C. Chavan, R.F. Bhajantri, M.S. Murari, Modification in the microstructure of sodium carboxymethylcellulose/polyvinyl alcohol polyblend films through the incorporation of NaNO3 for energy storage applications, Int. J. Energy Res. 46 (2022) 22845–22866.
[22] S.K. Shetty, Ismayil, I.M. Noor, Effect of new crystalline phase on the ionic conduction properties of sodium perchlorate salt doped carboxymethyl cellulose biopolymer electrolyte films, J. Polym. Res. 28 (2021) 415.
[23] R. Bakar, S. Darvishi, U. Aydemir, U. Yahsi, C. Tav, Y.Z. Menceloglu, E. Senses, Decoding polymer architecture effect on ion clustering, chain dynamics, and ionic conductivity in polymer electrolytes, ACS Appl. Energy Mater. 6 (2023) 4053–4064.
[24] S. Kumar, T. Demappa, J. Sannappa, Influence of KI salt concentration on the hydroxypropyl methylcellulose films: Optical study, Opt. Mater. (Amst). 129 (2022) 112474.
[25] Y. Ikemoto, Y. Harada, M. Tanaka, S. Nishimura, D. Murakami, N. Kurahashi, T. Moriwaki, K. Yamazoe, H. Washizu, Y. Ishii, Infrared spectra and hydrogen-bond configurations of water molecules at the interface of water-insoluble polymers under humidified conditions, J. Phys. Chem. B 126 (2022) 4143.
[26] A.H. Hassien, S.A. Salman, Preparation and Study of Structural, Optical and Electrical Properties of Composite Film [Pva-Peo-Mncl2. 4h2o], (n.d.).
[27] J.M. Hadi, B.K. Aziz, S.B. Aziz, Structural and electrochemical properties of ternary solid polymer electrolytes based on PVA: CS: FSG doped with sodium thiocyanate, Sci. Rep. 15 (2025) 14379.
[28] V. Cyriac, Ismayil, I.M. Noor, K. Mishra, C. Chavan, R.F. Bhajantri, S.P. Masti, Ionic conductivity enhancement of PVA: carboxymethyl cellulose poly-blend electrolyte films through the doping of NaI salt, Cellulose 29 (2022) 3271–3291. https://doi.org/10.1007/s10570-022-04483-z.
[29] J.P. Mendes, J. Esperança, M.J. Medeiros, A. Pawlicka, M.M. Silva, Structural, morphological, ionic conductivity, and thermal properties of pectin-based polymer electrolytes, Mol. Cryst. Liq. Cryst. 643 (2017) 266–273.
[30] J. Koliyoor, Ismayil, S. Hegde, G. Sanjeev, M.S. Murari, An insight into the suitability of magnesium ion-conducting biodegradable methyl cellulose solid polymer electrolyte film in energy storage devices, J. Mater. Sci. 58 (2023) 5389–5412.
[31] A. Gupta, D.K. Rai, Studies on sodium carboxymethyl cellulose+ sodium triflate polymer electrolyte, Energy Storage 6 (2024) e552.
[32] P.B. Bhargav, B.A. Sarada, A.K. Sharma, V.V.R.N. Rao, Electrical conduction and dielectric relaxation phenomena of PVA based polymer electrolyte films, J. Macromol. Sci. Part A 47 (2009) 131–137.
[33] S.I. Abdul Halim, C.H. Chan, J. Apotheker, Basics of teaching electrochemical impedance spectroscopy of electrolytes for ion-rechargeable batteries–part 1: a good practice on estimation of bulk resistance of solid polymer electrolytes, Chem. Teach. Int. 3 (2021) 105–115.
[34] M. Srinivas, R. Bhajantri, Strategy on enhancing ionic conductivity of biocompatible hydroxypropyl methyl cellulose/polyethylene glycol polymer blend electrolyte with TiO2 nanofillers and LiNO3 ionic salt, J. Electrochem. Sci. Eng. 14 (2024) 395–416.
[35] B.K. Faris, A.A. Hassan, S.B. Aziz, M.A. Brza, A.M. Abdullah, A.A. Abdalrahman, O.A. Abu Ali, D.I. Saleh, Impedance, electrical equivalent circuit (EEC) modeling, structural (FTIR and XRD), dielectric, and electric modulus study of MC-based ion-conducting solid polymer electrolytes, Materials (Basel). 15 (2021) 170.
[36] M. Sadiq, M.A. Khan, M.M. Hasan Raza, S.M. Aalam, M. Zulfequar, J. Ali, Enhancement of electrochemical stability window and

electrical properties of CNT-based PVA–PEG polymer blend composites, ACS Omega 7 (2022) 40116–40131.
[37] Y. Mallaiah, V.R. Jeedi, R. Swarnalatha, A. Raju, S.N. Reddy, A.S. Chary, Impact of polymer blending on ionic conduction mechanism and dielectric properties of sodium based PEO-PVdF solid polymer electrolyte systems, J. Phys. Chem. Solids 155 (2021) 110096.
[38] K. Arulraj, A.J. Sunija, Development and Property Evaluation of Sustainable Solid Polymer Electrolyte Based on Chitosan, Polyvinyl Alcohol and Polyvinyl Pyrolidone Blend Doped With NaNO3, Polym. Adv. Technol. 36 (2025) e70328.
[39] D. Kumar, K. Gohel, D.K. Kanchan, K. Mishra, Dielectrics and battery studies on flexible nanocomposite gel polymer electrolyte membranes for sodium batteries, J. Mater. Sci. Mater. Electron. 31 (2020) 13249–13260.
[40] A. Arya, A.L. Sharma, Structural, electrical properties and dielectric relaxations in Na+-ion-conducting solid polymer electrolyte, J. Phys. Condens. Matter 30 (2018) 165402.
[41] V. Cyriac, Y.N. Sudhakar, K. Mishra, Z.E. Rojudi, M.S. Murari, I.M. Noor, Effect of dopant on ion-dynamics of sodium ion-based flexible polyblend electrolyte for electrochemical device application, Mater. Res. Bull. 169 (2024) 112498.
[42] S. Kumar, S.R. Nagarajaiah, S. Raghu, S. Dongre, D. Thippaiah, S. Jadiyappa, Dielectric and conductivity study of salt-doped HPMC solid polymer electrolyte films, Biointerface Res. Appl. Chem. 13 (2023).
[43] S.B. Aziz, O.G. Abdullah, M.A. Rasheed, H.M. Ahmed, Effect of high salt concentration (HSC) on structural, morphological, and electrical characteristics of chitosan based solid polymer electrolytes, Polymers (Basel). 9 (2017) 187.
[44] M. Smiljanić, U. Petek, M. Bele, F. Ruiz-Zepeda, M. Šala, P. Jovanovič, M. Gaberšček, N. Hodnik, Electrochemical stability and degradation mechanisms of commercial carbon-supported gold nanoparticles in acidic media, J. Phys. Chem. C 125 (2021) 635–647.
[45] V. Gudihal, R.F. Bhajantri, C. Chavan, J.P. Pinto, K.H. Neha, Y. Patil, Synergistic influence of ZnO nanofillers and sodium alginate on ionic transport in PVA/NaCMC polymer electrolytes for primary battery systems, Ionics (Kiel). 32 (2026) 587–612.
[46] W.M. Dose, W. Li, I. Temprano, C.A. O'Keefe, B.L. Mehdi, M.F.L. De Volder, C.P. Grey, Onset potential for electrolyte oxidation and Ni-rich cathode degradation in lithium-ion batteries, ACS Energy Lett. 7 (2022) 3524.
[47] K.H. Neha, R.F. Bhajantri, S. Mohan, Influence of surface charged Al2. 67O4 nanofiller on conductivity and stability in plasticized green Hydroxypropyl Methylcellulose/Pectin incorporated with LiClO4 polymer composite electrolyte., J. Indian Chem. Soc. (2025) 101926.
[48] K.M.K. Yap, E.E. Abdo, H. Aramaki, H. Sugisawa, T. Hamamura, K. Mukunoki, J. Im, H. Celik, S.A. Hesse, P.P. Paul, Ion Transport and Crystal Rotation in Plastic Crystal Electrolytes Under Applied Electric Fields, Chem. Mater. (2026).
[49] Y. He, F. Ding, L. Lin, Z. Wang, Z. Lu, Y. Zhang, Influence of interfacial concentration polarization on lithium metal electrodeposition, Acta Phys.-Chim. Sin. 37 (2021) 2009001.
[50] J.P. Medina Flechas, D. Barrit, R.D. Patel, T. Li, E. Cariou, M. Provost, L. Kopprio, S. Le Gall, J.-P. Kleider, O. Almora, Characterization of ionic–electronic transport and recombination in perovskite solar cells under multi-biasing conditions, EES Sol. (2026).
[51] X. Shan, M. Morey, Z. Li, S. Zhao, S. Song, Z. Xiao, H. Feng, S. Gao, G. Li, A.P. Sokolov, A polymer electrolyte with high cationic transport number for safe and stable solid Li-metal batteries, ACS Energy Lett. 7 (2022) 4342–4351.